地 震 研 究 所 彙 報
Bull. Earthq. Res. Inst.
Univ. Tokyo
Vol. 81 (2006) pp. 295–301

# Estimation of 3D S-wave Velocity Model of the Kanto Basin, Japan, Using Rayleigh Wave Phase Velocity

Hiroaki Yamanaka[1)]* and Nobuyuki Yamada[2)]

[1)] Department of Environmental Science and Technology, Tokyo Institute of Technology, Yokohama, Kanagawa 226–8503, Japan

[2)] Fukuoka University of Education, Munakata city, Fukuoka 811–4192, Japan

**Abstract**

Microtremor array explorations were conducted in the Kanto basin, Japan, to obtain Rayleigh wave phase velocity in a long-period range to estimate S-wave velocity profiles down to the basement having an S-wave velocity of about 3 km/s. Rayleigh wave phase velocity data in the previous surveys in the area were used to estimate thicknesses of 3 layers of the sedimentary layers with the same conditions, such as numbers of layers and S-wave velocity in the 1D inversion. The 1D S-wave velocity profiles at 241 sites were used to construct a 3D S-wave velocity model of the basin. Synthetic long-period ground motion for a moderate shallow earthquake is calculated using the estimated 3D basin model. We found a better fitting of the synthetics with observed ground motion than that for the previous 3D model.

**Key words** : Kanto basin, microtremors, Rayleigh wave, S-wave velocity exploration, ground motion

## 1. Introduction

Engineering requirements to know characteristics of strong ground motion in a period range longer than 1 second have been increased since 70s with an increase in numbers of large-scaled structure, such as tall buildings, long-spanned bridges, and large oil storage tanks. The importance of the lone-period strong motion was again recognized during the 2003 Tokachi-oki earthquake in Japan, when large oils tanks in Tomakomai were fired possibly due to sloshing of flammable liquid. It is indicated that ground motion in the city of Tomakomai is rich in long-period components with a dominant period of about 7 seconds, because the city is located in a large basin (e.g., Hatayama *et al.,* 2005).

S-wave velocity distribution from the surface to the basement with an S-wave velocity of about 3 km/s is one of the most important parameters to control characteristics of long-period motion. In particular, 3D S-wave velocity structure of deep sedimentary layers must be accurately prepared to simulate complex wave field of ground motion at a site in a basin. Among many geophysical explorations for S-wave velocity distribution, it is recognized that the microtremor array technique is the most powerful and economic technique to know an S-wave velocity profile of a deep basin (e.g., Horike, 1985). In the method, Rayleigh wave phase velocity in a long-period range up to several seconds is used to estimate an S-wave velocity profile. Since the wave type and the period range used in the microtremor array exploration is the same as those interested in strong motion estimation. This feature can be regarded as one of the advantages of the methods over the other geophysical exploration techniques.

In this study, we conducted microtremor array explorations at 34 sites in the Kanto basin, Japan to estimate 1D S-wave velocity profiles of deep sedimentary layers over the basement. Rayleigh wave phase velocity data at 207 sites in previous explorations were also collected to invert them to 1D S-wave velocity profiles with the same assumptions. Combining the inverted profiles at all the sites, a new 3D S-wave velocity model for the Kanto basin is con-

* e-mail: yamanaka@depe.titech.ac.jp

structed. Synthetic earthquake ground motion was calculated for the 3D model with a finite difference simulation technique to investigate its performance.

## 2. Microtremor explorations

Microtremor explorations have been conducted in the Kanto plain by several researchers (e.g., Kanno, 2000, Matsuoka *et al.,* 2002 ; Yamanaka *et al.,* 2000 ; Yamanaka and Yamada, 2002) and local governments, such as Tokyo Metropolitan government, Kanagawa and Chiba prefectures, and Yokohama and Kawasaki cities. Some of private companies also conducted for providing basic information of subsurface structure in seismic design of buildings. The locations of the sites in the previous explorations are shown by solid circles in Fig. 1. It is clear from the figure that they are concentrated in central and southwestern parts of the basin. We, therefore, conducted similar microtremor array explorations at 34 sites in the northern and eastern parts to cover whole of the basin. Two to three temporary arrays with station intervals of 0.3 to 2 km were deployed at each site by installing 7 vertical seismometers to obtain simultaneous array records of microtremors.

Frequency-wavenumber spectral analysis (Capon, 1960) was applied to the array records to estimate Rayleigh wave phase velocity in a period range approximately from 0.5 to 5 seconds. Examples of the phase velocities estimated at the sites along the line C-C′ are shown in Fig. 2. The phase velocity at KYN becomes large at periods longer than 1.8 seconds suggesting shallow basement depth. The phase velocity at each site was inverted to a 1D S-wave velocity profile. A genetic algorithm (Yamanaka and Ishida, 1996) is used to find a model with the minimum misfit between observed and theoretical phase velocities of fundamental Rayleigh wave. Four-layer model is assumed according to previous research (e.g., Yamanaka and Yamada, 2002). The S-wave velocity profiles inverted from the phase velocities in Fig. 2 are shown in Fig. 3. The profiles exhibit basin-like features of the basement depth. We estimated S-wave velocity profiles from phase velocity at all the 34 sites in the similar way.

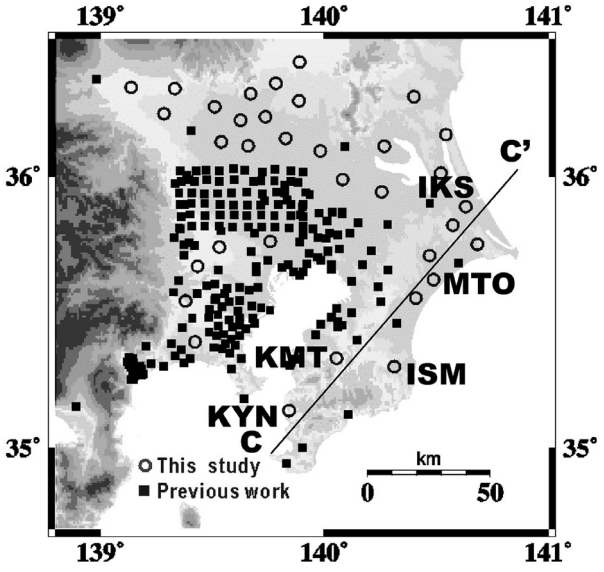


Fig. 1. Locations of microtremor array explorations in this study (circles) and previous studies (squares).

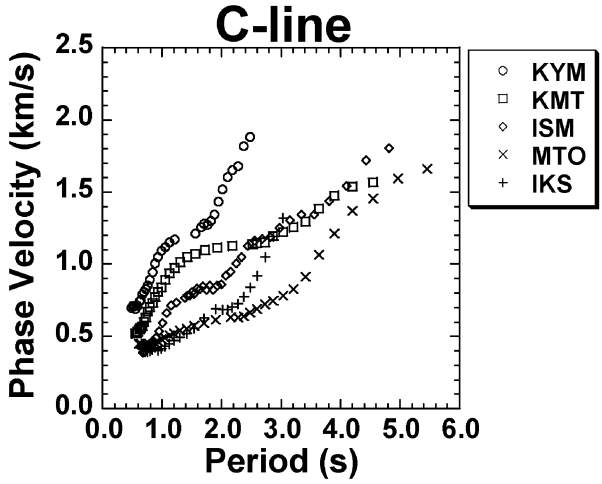


Fig. 2. Rayleigh wave phase velocity at sites along line C-C′ in Fig. 1.

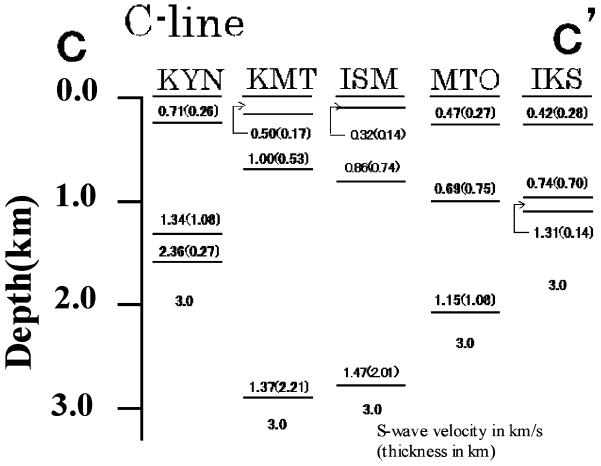


Fig. 3. S-wave velocity profiles from individual inversions of phase velocity in Fig. 2.

### 3. Spatial distribution of phase velocity

Rayleigh wave phase velocities obtained at 207 sites in the previous microtremor explorations were collected to combine with the phase velocity data in this study in the further analysis. Totally we could use the phase velocities at the 241 sites in the basin as shown in Fig. 1. Since the period range and interval of the phase velocities collected are not the same, we interpolated the phase velocity at each site at the same period interval. Figures 4 and 5 shows the average and the standard deviation of the Rayleigh wave phase velocity. The phase velocity was obtained in a period range from 0.6 to 5 seconds at many sites. The number of the data is not enough at periods of more than 5 seconds. Probably, this is due to a reduction of the spectral power of microtremors in the period range. The standard deviation is large in a period range from 1 to 5 seconds, suggesting the wide variation of the phase velocity. Spatial variation of the Rayleigh wave phase velocity at periods of 3.1 and 1.0 seconds are shown in Fig. 6. The phase velocity at periods of 3.1 seconds is very low in the eastern parts of the basin with a phase velocity of 1 km/s. On the other hand, the phase velocity at 1

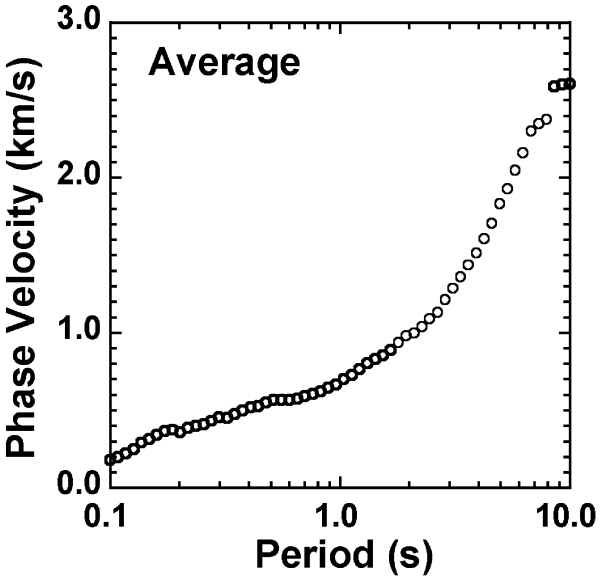


Fig. 4. Average phase velocity of Rayleigh wave at all the sites in Fig. 1.

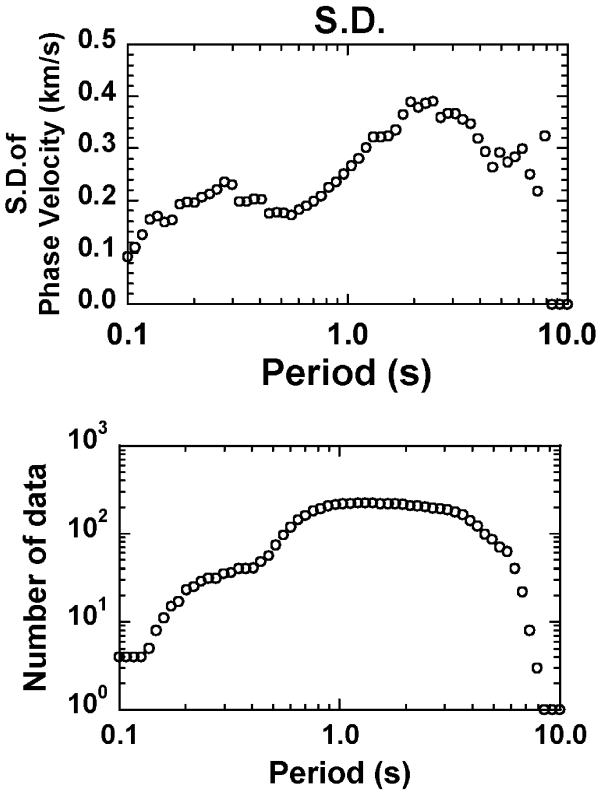


Fig. 5. Standard deviation of phase velocity of Rayleigh wave with data number used in calculation.

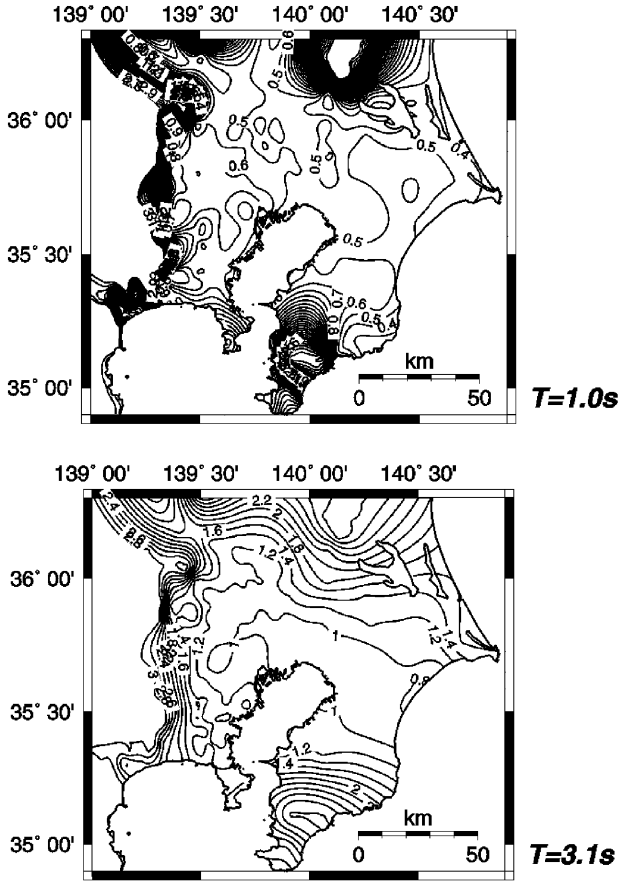


Fig. 6. Distributions of Rayleigh-wave phase velocity at periods of 3.1 (bottom) and 1.0 seconds (top) from microtremor array explorations.

second is low in the central part.

## 4. Construction of 3D basin model

The phase velocities obtained in the previous explorations have been already inverted to 1D S-wave profiles using inversion methods or forward modeling. However, assumptions and constraint conditions in the inversions of the phase velocity are significantly different in each exploration. This makes it difficult to unify the results of all the explorations for constructing a 3D basin model. Therefore, we again invert all the collected phase velocities with the same assumptions.

Yamanaka and Yamada (2002) used three-layer models of the sediments over the basement in the inversions of Rayleigh-wave phase velocity from microtremor explorations in the area. It is assumed in their study that the top layer corresponds to Quaternary layer and the second and third layers belong to Tertiary age. We also assumed such four layers in the inversions of all the phase velocity data. Thickness of each layer and S-wave velocity of the top layer are selected as unknown parameters in the inversions. The S-wave velocities for the second, third and bottom layers are assumed to be 1.0, 1.5 and 3.0 km/s, respectively. These S-wave velocities are approximately the average values of results of the individual phase velocity inversions. P-wave velocity is calculated from S-wave velocity using an empirical relation. Density is given in advance. Although the assumption of the constant S-wave velocity constrains the inversion so much, this makes it easy to integrate inversion results for a 3D model. We again used the genetic inversion (Yamanaka and Ishida, 1996).

The S-wave velocity profiles at the sites along the C-C′ line are displayed in Fig. 7. Although the depths to the basement in the profiles in the figure are similar to those in Fig. 3, the depths to the intermediate layers differ from each other, because of the constraint conditions on the S-wave velocity. The S-wave velocities in the top layer are the almost the same as the models in Fig. 2. This clearly indicates a strong lateral variation in the basin, and should be taken into account in short-period surface wave propagation.

After we obtained the depths to the three interfaces at all the sites from the above inversions, these data were used in a construction of a new 3D S-wave velocity model for the basin. Figure 8 shows the

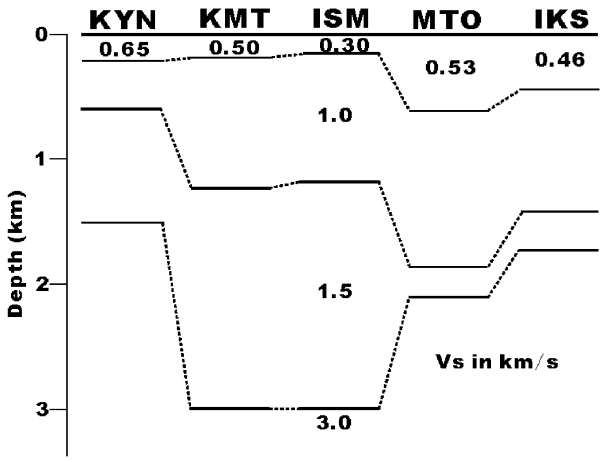


Fig. 7. S-wave profiles inverted from phase velocities in Fig. 2 with assumption of constant S-wave velocities except for that of top layer.

maps to the depths of the top of the layers having S-wave velocities of 1.0, 1.5, 3.0 km/s. We assumed the existence of no sedimentary layers in the mountain area in drawing the maps. It is also noted that the subsurface structure for the Sagami bay area in the south-off of the basin is almost the same as estimated by Yamanaka and Yamada (2002). The depth contour shown by broken lines corresponds to this area. The thickness of the top layer in Fig. 8a (depth to the second layer) is the thickest in the north of the Tokyo bay and thin in the marginal parts of the basin. The depths to the third layer also show the deepest point in the similar part as can be seen in Fig. 8b. However, the basement depth in Fig. 8c is the deepest at the eastern coast of the Tokyo bay in the Chiba prefecture. We can also see the deep and narrow valley in the northwestern part of the basin with a depth more than 3 km. The distribution of the S-wave velocity of the top layer is shown in Fig. 8d. The S-wave velocity is larger in the southwestern part than that in the other part.

Figure 9 shows the basement depth map proposed by Yamanaka and Yamada (2002) from compiling S-wave velocity profiles from microtremor exploration. Because their used data were not densely distributed as explained earlier, the depth contours are simpler than those in Fig. 8c. The locations with the largest basement depth in the two models are different.

## 5. FD Simulation of earthquake ground motion

We, here, calculated synthetic earthquake ground

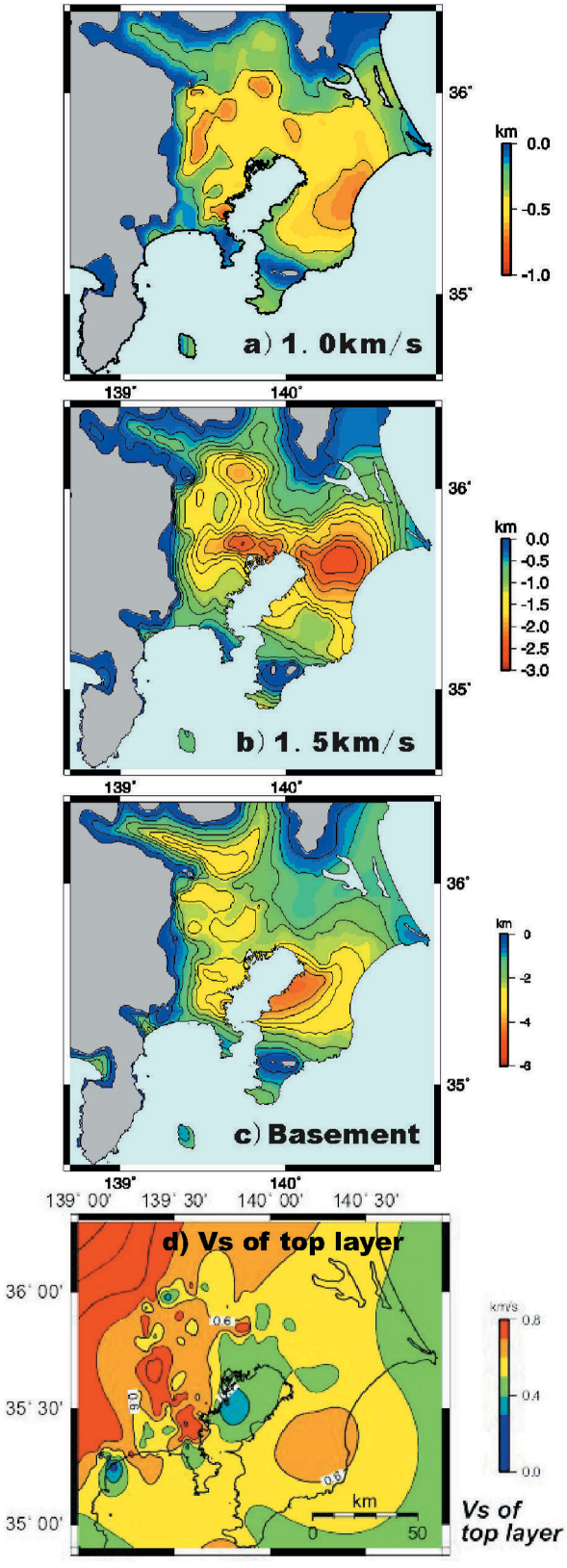


Fig. 8. Three-dimensional S-wave velocity model of the Kanto basin. The depths to the top of the layers having S-wave velocities of (a) 1.0, (b) 1.5 and (c) 3.0 km/s are displayed with (d) variation of the S-wave velocity of the top layer.

motion due to a moderate event around the basin in order to understand performance of the constructed 3D basin model. The target event is shallow one occurred on 20, Feb. 1990 near Izu-Oshima with an Mj of 6.5. The locations of epicenter and observation stations are shown in Fig. 10. Yamada and Yamanaka (2000) calculated the synthetic motion for the event with a three-dimensional finite difference method and compared with the observed motion at the stations. Their 3D basin model was also based on results of microtremor array explorations by Yamanaka and Yamada (2002). However, their data are significantly less than those used in this study.

The FD code used is the same as Yamada and Yamanaka (2000). The equation motion in the velocity-stress representation is discredited with accuracy of 4th order in space and 2nd order in time. The basin and surrounding areas with a size of E 220 km, N 200 km, Z 140 km are digitized into grind points. The sedimentary layers over the basement are discredited with a grid mesh of 400 meters, while the subsurface structure of the Crust and the Mantle is modeled with a rectangular grid mesh in which the grid interval in the depth direction is 2.5 times larger than those of the horizontal directions. Constant Q-values calculated from Vs (m/s)/5 to Vs/10 are assumed for all the layers. We used a smoothed ramp

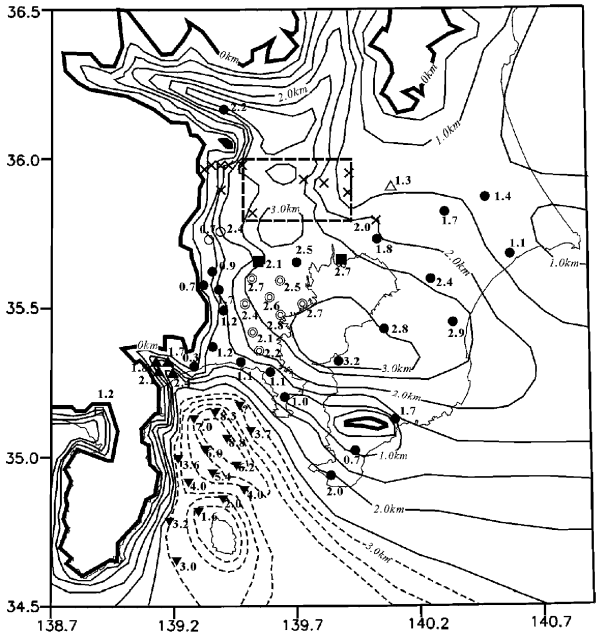


Fig. 9. Basement depth map proposed by Yamanaka and Yamada (2002).

function with irregular slips in the fault plane estimated in Fukuyama and Mikumo (1993).

The calculated ground velocities at the surface of the basin models in this study and by Yamanaka and Yamada (2002) are shown together with the observed velocities in Fig. 11. Although the observed ground motions were not completely reconstructed by the FD computation using the two models, the synthetic motion for our model fits the observed motion better than that for the previous model. In particular, the characteristics of the east-west oriented ground velocities observed at TOK (Tokyo) and YKH (Yokohama) are well simulated by the computation for the new model. We also compared the computed results with the observation in frequency domain. Figure 12 shows velocity response spectra of the synthetic and observed motions at TOK, YKH, and NRS. The observed spectral shapes are almost in agreement with the calculated ones at TOK and YKH. The spectrum at NRS calculated for our model is also much similar to the observed one than that for the previous model. The distributions of the peak ground velocity in the east-west direction are also compared in Fig. 13. The distributions are difference from each other. The spatial variation for the new model is much larger than that of the previous model, indicating the high-resolution of the sediment depths in our model.

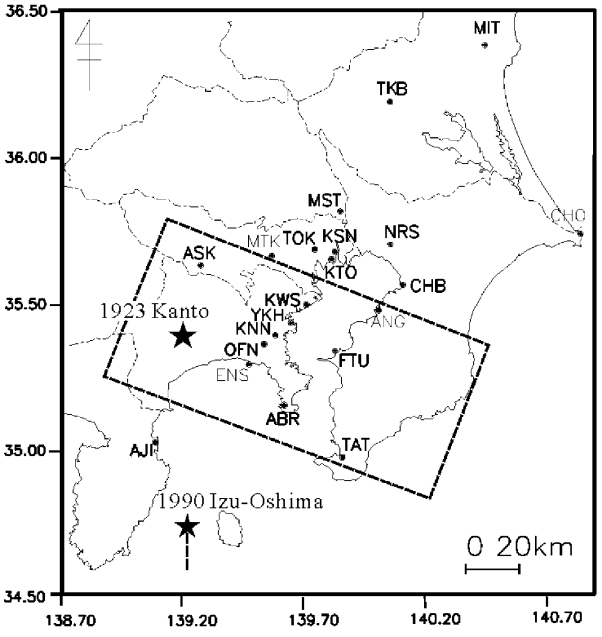


Fig. 10. Locations of earthquake observation stations during the earthquake of 20, Feb. 1990 near Izu-Oshima. The squared area indicates the fault plane of the 1923 Kanto earthquake.

## 6. Conclusions

A new 3D S-wave velocity model of the Kanto basin was constructed using Rayleigh wave phase velocities estimated in microtremor explorations at more than 200 sites. Performance of the new model was investigated with a comparison with the ground motions observed during a moderate shallow earthquake. The synthetic motion for the model fits better with the observed ones than that of the previous model.

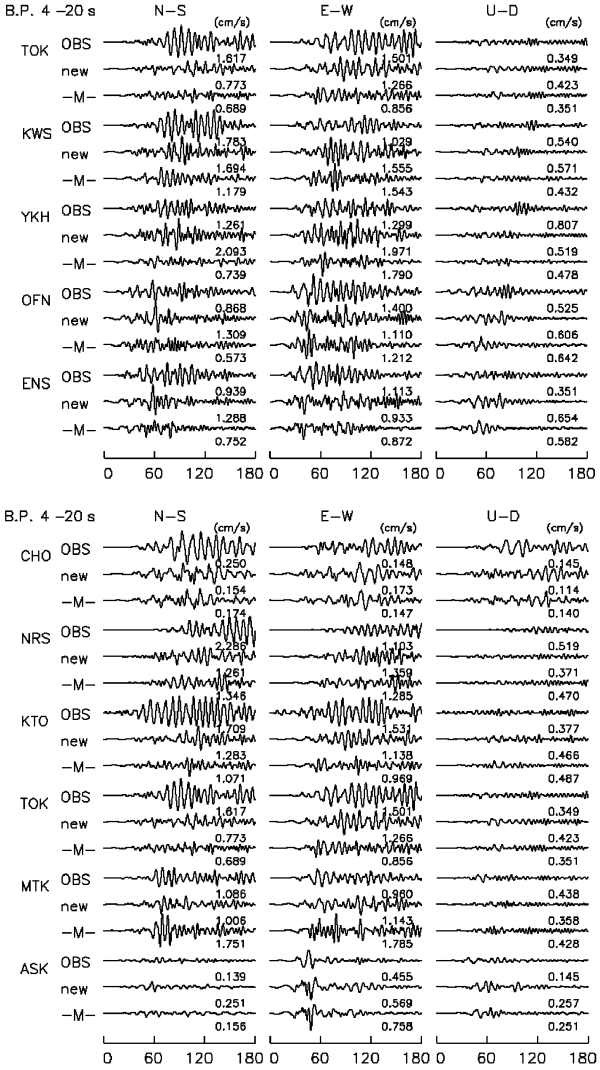


Fig. 11. Comparison of observed ground velocities (top) with synthetic ground velocities from FD simulation using basin models in this study (middle) and previous study by Yamanaka and Yamada (2002) (bottom). Traces are filtered with period range from 4 to 20 sec.

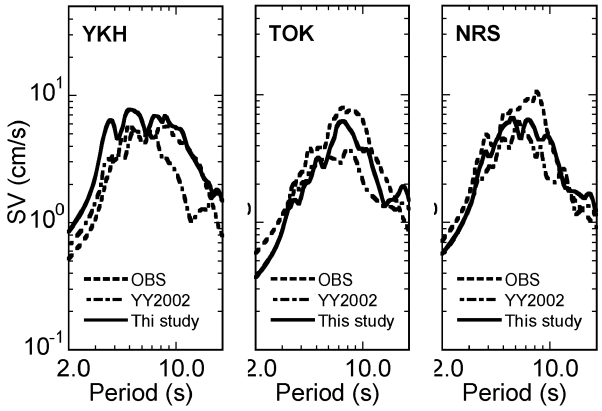


Fig. 12. Comparison of observed response spectra (h =5%) with synthetic ones in east-west direction from FD simulation using basin models in this study and previous study by Yamanaka and Yamada (2002) as noted YY2002.

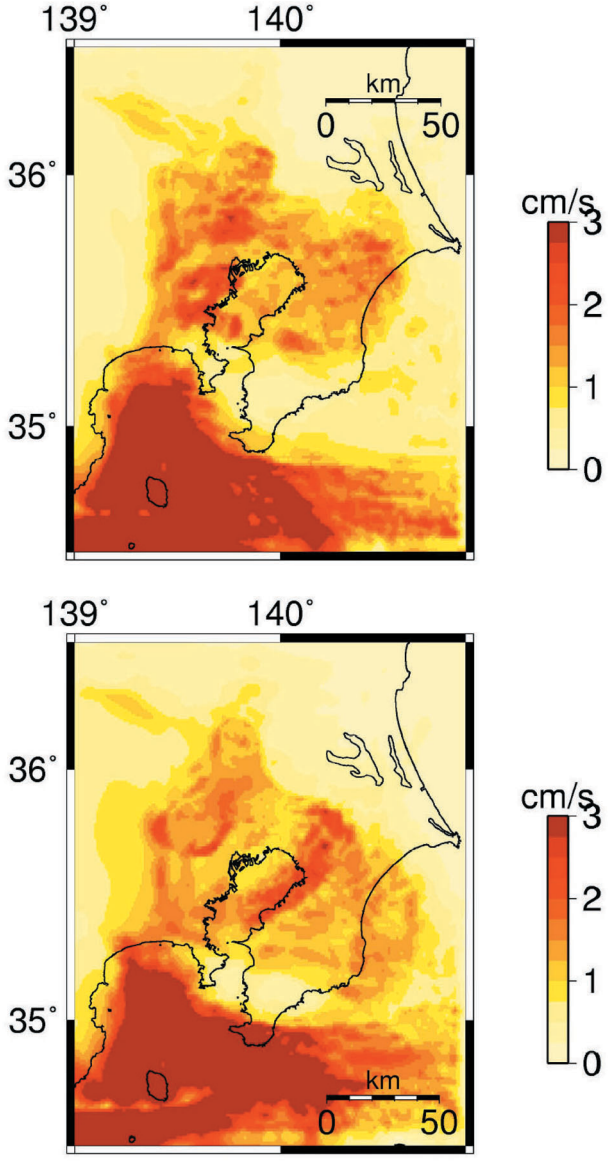


Fig. 13. Distributions of PGV for east-west oriented synthetic ground motions for basin models in this study (top) and previous study by Yamanaka and Yamada (2002) (bottom).

**Acknowledgments**

We thank Nobuhiko KOMABA for discussion and help during the research. We also thank those who provide phase velocity data to us. A part of the phase velocity data were provided from Tokyo Metropolitan government, Kanagawa and Chiba prefectures and Yokohama and Kawasaki cities.

**References**

Capon, J. (1969). High resolution frequency wavenumber spectrum analysis, *Proc. I.E.E.E.,* 57, 1408–1418.

Fukuyama, E. and T. Mikumo (1993). Dynamic rupture analysis : Inversion for the source process of the 1990 Izu-Oshima, Japan, Earthquake (M=6.5), *J. Geophys. Res.,* 84, 6529–6542.

Hatayama, K., *et al.* (2005). Long-period ground motion and damage to oil storage tanks due to the 2003 Tokachi-oki earthquake, *Zisin* (Jour. Seis, Soc. Japan), 57, 83–103 (in Japanese).

Horike, M. (1985). Inversion of phase velocity of long-period microtremors to the S-wave velocity structure down to the basement in urbanized area, *Jour. Phys. Earth,* 33, 59–96.

Kanno, T. (2000). A study on design input motion considering deep subsurface structure, PhD thesis, Univ. of Tokyo, 1–164 (in Japanese).

Matsuoka, T and Shiraishi H. (2002). Application of an exploration method using microtremor array observation for high resolution survey of deep geological structure in the Kanto plains, *Butsuri-Tansa,* 55, 127–143 (in Japanese).

Yamanaka H. and Ishida H. (1996). Application of genetic algorithms to an inversion of surface-wave dispersion data, *Bull. Seis. Soc. Am.,* 86, 436–444.

Yamanaka,H., *et al.* (2000) Exploration of basin structure by microtremor array technique for estimation of long-period ground motion. *12th World Conf. Earthq. Eng.* CDROM, No.1484.

Yamanaka, H. and N. Yamada (2002). Estimation of 3D S-wave velocity model of deep sedimentary layers in Kanto plain, Japan, using microtremor array measurements, *Butsuri-Tansa* (Geophysical exploration), 55, 53–66 (in Japanese).

Yamada N. and H. Yamanaka (2000). Three-dimensional finite difference simulation of long-period ground motion in the Kanto plain, Japan, *12th World Conf. Earthq. Eng,* CDROM, NO.1486.

(Received December 5, 2005)
(Accepted November 14, 2006)